

Fröhlich-interaction-induced multiphonon Raman scattering in SrCuO_2 and $\text{Sr}_{0.5}\text{Ca}_{0.5}\text{CuO}_2$

M. V. Abrashev,* A. P. Litvinchuk, and C. Thomsen

Institut für Festkörperphysik, Technische Universität Berlin, Hardenbergstrasse 36, D-10623 Berlin, Germany

V. N. Popov

Faculty of Physics, Sofia University, BG-1126 Sofia, Bulgaria

(Received 21 November 1996)

Polarized Raman spectra of $\text{Sr}_{1-x}\text{Ca}_x\text{CuO}_2$ ($x=0, 0.5$) microcrystals were studied experimentally. In addition to the Raman-allowed modes, we observed numerous lines with A_g symmetry and frequencies up to 2400 cm^{-1} , which appear only for polarizations parallel to the chains. We show that this additional Raman scattering originates from the three infrared-active-only B_{1u} LO modes and their overtones and combinations, becoming Raman active via Fröhlich interaction. [S0163-1829(97)51414-7]

The interest in the orthorhombic cuprates Sr_2CuO_3 and SrCuO_2 containing single and double copper-oxygen chains, respectively, has increased considerably after it was found that these structures are almost ideal one-dimensional (1D) spin-1/2 antiferromagnets.^{1,2} The exchange interaction energy J was estimated from magnetic susceptibility measurements to be 2200 K and 2100 K, respectively.² The analysis in terms of the phonon-assisted absorption in the one-dimensional quantum spin chain model of a structure observed at 0.48 eV in the midinfrared absorption spectrum of Sr_2CuO_3 , obtained for polarization along the chains, suggests a similar value of J .³

Recently, in a Raman investigation of Sr_2CuO_3 and SrCuO_2 single crystals, many forbidden peaks superimposed on a strong continuum were observed in addition to the Raman-allowed phonons in spectra polarized along the Cu-O chains.⁴ Part of these additional features were ascribed either to phonons strongly coupled to spinons or to spinon-spinon pairs. Similar Raman-scattering peaks were observed earlier in $\text{Ca}_{2-x}\text{Sr}_x\text{CuO}_3$ compounds which are isostructural to Sr_2CuO_3 .^{5,6} In Ref. 5 these additional lines were assigned to zone-boundary phonons, activated by the Ca,Sr disorder, and their combinations. In Ref. 6, based on a comparison with the calculated two-phonon density of states, these lines were attributed to resonantly enhanced two-phonon scattering.

The same phenomenon was observed in the Raman spectra of insulating layered cuprates when the polarization is parallel to the Cu-O planes and the incident laser energy is close to the charge-transfer gap energy (1.8–2 eV).^{7–11} Sugai⁷ showed in the case of $\text{La}_{2-x}\text{Sr}_x\text{CuO}_4$ that the intensity of the additional peaks decreases with increasing Sr content x and interpreted this dependence as an indication of the lower symmetry of the parent compound ($x=0$). Heyen *et al.*,⁸ in a study of the one-phonon region of the Raman spectra of $\text{YBa}_2\text{Cu}_3\text{O}_6$ under resonant conditions, observed that the frequencies of all additional lines in the xx spectra coincided with those of infrared-active only E_u LO phonons of the structure. The polarization and resonance behavior, as well as the relative intensity of these lines supported a Fröhlich model of activation of these modes. Moreover, it was explained that a relatively low concentration of crystal imperfections (every several hundred unit cells) is sufficient to

make this scattering independent of the direction of wave-vector transfer (i.e., a breakdown of the momentum conservation rule).

Yoshida *et al.*⁹ investigated the main members of the three types of insulating cuprates with a different oxygen coordination of copper, namely, $\text{Ca}_{0.85}\text{Sr}_{0.15}\text{CuO}_2$ (fourfold), $\text{YBa}_2\text{Cu}_3\text{O}_6$ (fivefold) and La_2CuO_4 (sixfold) in a wide spectral and incident photon-energy range. They proposed that the origin of the additional lines is one-phonon scattering of the zone-boundary bending and stretching vibrations of the oxygen atoms in the Cu-O plane and their combinations. It is unclear, however, how zone-boundary phonons can take part in one-phonon Raman scattering. Considering only the highest-frequency line appearing in the $1000\text{--}1500\text{ cm}^{-1}$ region for layered cuprates with different Cu-O distances, Uzunaki *et al.*¹⁰ showed a clear correlation between the frequency of this line and the doubled frequency of the E_u LO Cu-O stretching mode. Reedyk *et al.*,¹¹ in a study of Raman spectra of $\text{Pb}_2\text{Sr}_2\text{PrCu}_3\text{O}_8$ under resonant conditions, assigned the observed resonating lines as Fröhlich-interaction-induced LO infrared-active modes and their combinations. Tuning the incident laser energy across the charge-transfer gap, they observed a change in the energy of the highest two-LO peak in agreement with the theory for two-LO-phonon resonant Raman scattering.

A study of the optical phonons in $\text{Sr}_{1-x}\text{Ca}_x\text{CuO}_2$ ($x=0, 0.5$) using micro-Raman and far-infrared spectroscopy and a comparison of the observed modes with lattice-dynamics calculations was made in Ref. 12. Here we resolve the issue about the origin of the additional strong Raman-forbidden lines up to 2400 cm^{-1} in the zz spectra of these compounds. We prove that all these lines originate from the three B_{1u} LO infrared-active modes and their combinations, becoming Raman-active via Fröhlich interaction. The temperature dependence of these lines is also discussed.

The synthesis and the characterization of the $\text{Sr}_{1-x}\text{Ca}_x\text{CuO}_2$ ceramics, consisting of microcrystals with sufficiently large dimensions for micro-Raman measurements, were described elsewhere.¹² The Raman spectra in backscattering configuration were obtained using a single spectrometer LABRAM, equipped with a microscope, a CCD multichannel detector and appropriate notch filters. A

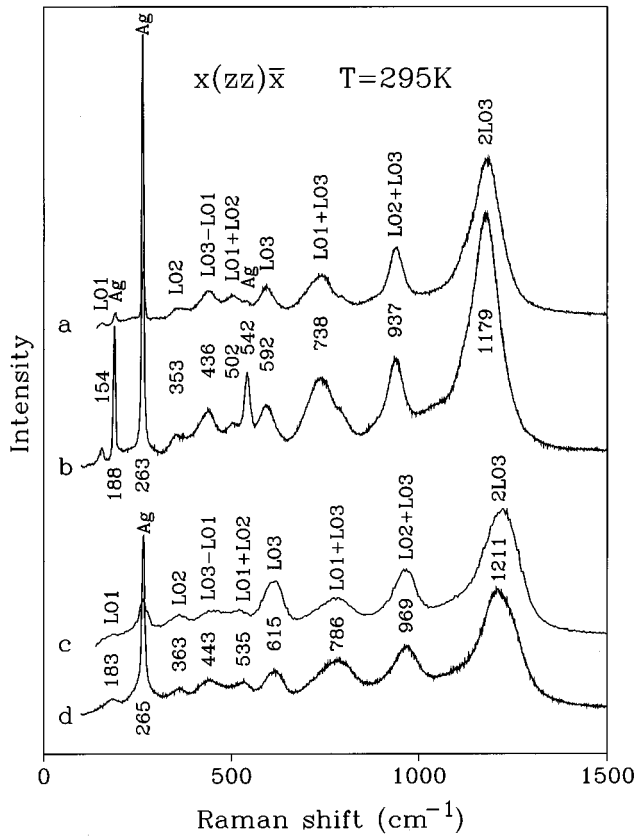


FIG. 1. $x(zz)\bar{x}$ Raman spectra at room temperature of (a) SrCuO_2 , $\lambda_L=514.5$ nm; (b) SrCuO_2 , $\lambda_L=632.8$ nm; (c) $\text{Sr}_{0.5}\text{Ca}_{0.5}\text{CuO}_2$, $\lambda_L=514.5$ nm; (d) $\text{Sr}_{0.5}\text{Ca}_{0.5}\text{CuO}_2$, $\lambda_L=632.8$ nm.

600 and an 1800 grooves/mm grating was used for the different spectral ranges investigated. The 632.8 nm He-Ne and 514.5 nm Ar^+ laser lines were used for excitation. For the low-temperature measurements the samples were mounted on a cold finger in a He-gas-flow cryostat.

The structure of the investigated isostructural compounds is orthorhombic, space group $Cmcm$.^{13,14} It contains double Cu-O chains separated by double rocksalt Sr-O layers. The x direction is in the plane of the rocksalt layer and perpen-

dicular to the chains, the y direction is perpendicular to the rocksalt layer, and the z direction is parallel to the chains. The identification of the orientation of the observed microcrystal surfaces and the corresponding crystal directions were determined by means of their crystal (needlelike shape) and optical (change in color) anisotropy as well as the available information about the polarization behavior of the first-order Raman-allowed modes.¹²

The spectra obtained in zz polarization parallel to the chains from SrCuO_2 and $\text{Sr}_{0.5}\text{Ca}_{0.5}\text{CuO}_2$ with two different laser lines are presented in Fig. 1. As was pointed out in Refs. 4,12, solely in spectra with zz polarization can numerous lines superimposed on a strong background be observed. Out of the four A_g modes existing in these compounds and tabulated in Ref. 12, we observed three in the zz spectra for SrCuO_2 and only one for $\text{Sr}_{0.5}\text{Ca}_{0.5}\text{CuO}_2$ (indicated in Fig. 1). The other peaks are symmetry forbidden. It is natural to propose that the nature of the additional peaks in the chained and in the layered cuprates is one and the same, i.e., Fröhlich-interaction-induced LO modes and their combinations. The analogs of E_u LO infrared-active modes (vibrations in the Cu-O planes), which are the origin of these lines in the layered cuprates,^{8,10,11} in our case are the B_{1u} LO infrared-active modes (vibrations along the chains). There are three such modes in $\text{Sr}_{1-x}\text{Ca}_x\text{CuO}_2$,¹² denoted here as LO1, LO2, and LO3. Indeed, three of the lines observed in Fig. 1 have frequencies very close to those of the B_{1u} LO modes. The remaining lines are sums or differences of these three lines (see Table I).

In Fig. 2 the $x(zz)\bar{x}$ spectra of SrCuO_2 obtained at different temperatures and for two laser excitation energies are presented. It is seen that only the peak at 436 cm^{-1} disappears at low temperatures. This confirms its two-phonon difference origin. We note also, that with decreasing temperature the band at 738 cm^{-1} looks more like a triple structure. Whereas the lower frequency shoulder near 700 cm^{-1} could be the 2LO2 line, the line at 790 cm^{-1} cannot be a combination of the three B_{1u} LO modes. The same holds for the weak line at 1060 cm^{-1} (observable at low temperatures only).

As was mentioned by Misochko *et al.*,⁴ the intensity of some peaks anomalously increases upon sample cooling. We

TABLE I. Frequencies (in cm^{-1}) and an assignment of the observed but not Raman-allowed peaks in the zz Raman spectra compared with the B_{1u} LO modes from a Kramers-Kronig analysis of the far-infrared reflectivity spectra (FIR) and lattice-dynamics calculations (LDC). In parentheses the corresponding combinations of the experimental one-phonon frequencies are listed.

Assignment	SrCuO_2			$\text{Sr}_{1-x}\text{Ca}_x\text{CuO}_2$		
	This paper	FIR Ref. 12	LDC	This paper	FIR Ref. 12	LDC
LO1	154	154	158	183	182	174
LO2	353	370	384	363	366	403
LO3	592	561	563	615	563	588
LO3 - LO1	436 (438)			443 (432)		
LO1 + LO2	502 (507)			535 (546)		
LO1 + LO3	738 (746)			786 (798)		
LO2 + LO3	937 (945)			969 (978)		
2LO3	1179 (1184)			1211 (1230)		

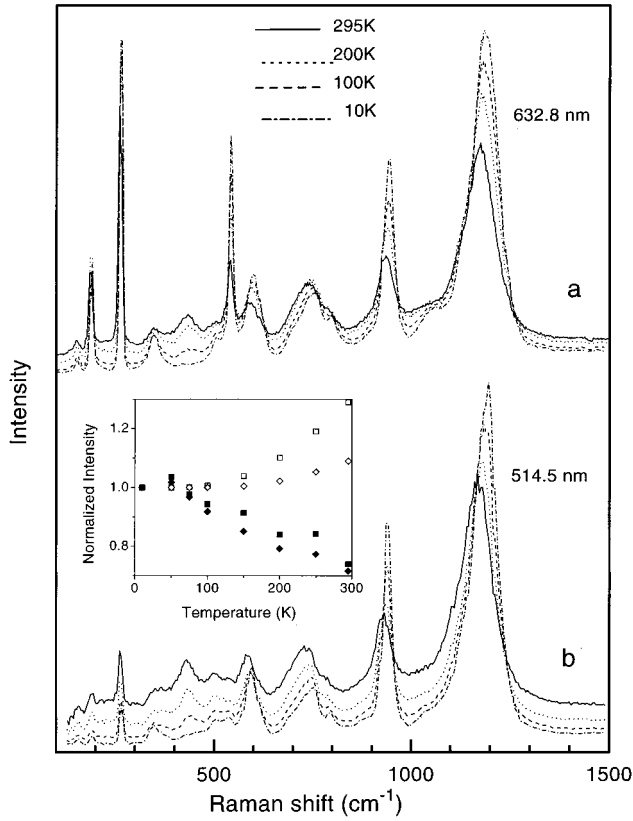


FIG. 2. $x(zz)\bar{x}$ Raman spectra of SrCuO_2 at different temperatures for (a) $\lambda_L = 632.8$ nm; (b) $\lambda_L = 514.5$ nm. The inset shows the temperature dependence of the intensity for the 937 cm^{-1} (squares) and 1179 cm^{-1} (diamonds) peaks. Open and black symbols are theoretical and experimental values, respectively.

confirmed this observation. In the set of spectra obtained using the 514.5 nm laser line, the peaks at 592 , 937 , and 1179 cm^{-1} clearly demonstrate such unexpected temperature behavior [see Fig. 2(b)]. In the inset of Fig. 2 the integrated intensities (normalized to 10 K) for the 937 and 1179 cm^{-1} lines are compared with the theoretical values (having accounted for the phonon occupation number only). To eliminate the error caused by different laser-spot focusing conditions, we used the intensity of the 263 cm^{-1} A_g line for internal normalization. However, we note that in the set of spectra obtained with 632.8 nm excitation, the three A_g lines show such increased intensity at low temperatures, too.

We will make an attempt to qualitatively explain this anomalous temperature dependence, especially for the two-phonon LO lines. The theoretical expression for the efficiency of two-LO-phonon resonant Raman scattering may be written as [see Eq. (25) from Ref. 15)]

$$\left(\frac{dS}{d\Omega}\right)_{2LO} = S_0 [N(\omega_{LO}) + 1]^2 \int_0^\infty dQ \frac{1}{Q^2} |F(Q)|^2, \quad (1)$$

where the integrand is dimensionless ($Q = qa$, q - the magnitude of the phonon wave vector, a - the exciton Bohr radius), $N(\omega_{LO})$ is the LO-phonon occupation number, S_0 is a product of fundamental constants and multipliers, weakly dependent on temperature, and $F(Q)$ is a sum of functions

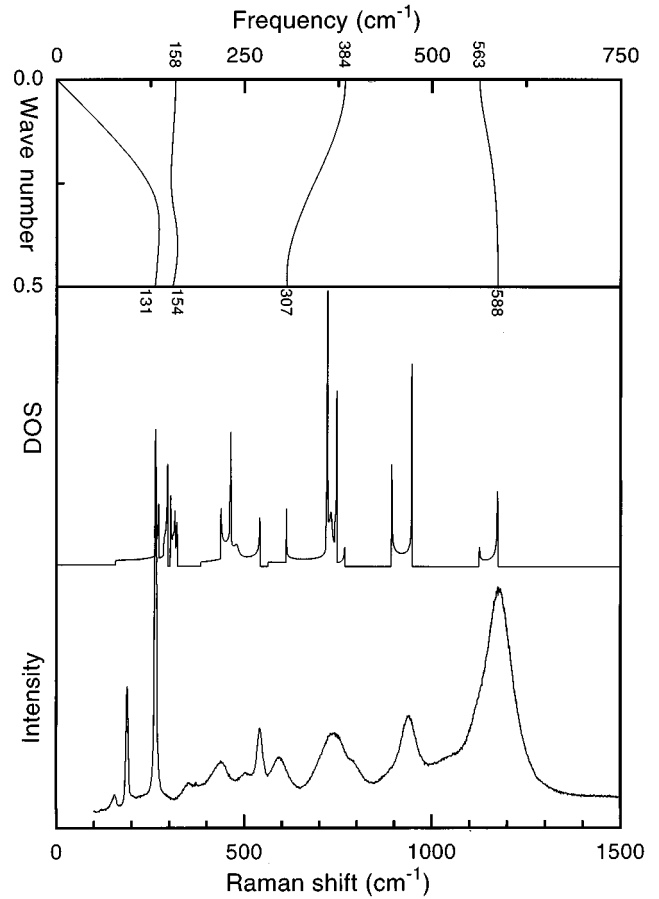


FIG. 3. Calculated phonon-dispersion curves in z ($0,0,k$) direction beginning from the three LO and the acoustical modes with B_{1u} symmetry at the Γ point (upper panel). The calculated combination two-phonon density of states using only these four dispersion curves (middle). A $x(zz)\bar{x}$ Raman spectrum of SrCuO_2 , $T = 295$ K, $\lambda_L = 632.8$ nm (bottom).

corresponding to different types of intermediate states for the scattering process. For real crystals, however, the integrand Q is defined only for values between $Q_{min} \sim a/l$ (l - the mean free phonon path) and $Q_{max} \sim a/c$ (c - the lattice parameter). With decreasing temperature l increases and the value of the integral will increase rapidly due to the factor $1/Q^2$. It appears that the intensity of this scattering correlates with the mean free path of the corresponding phonons. We also expect a correction due to the temperature dependence of the electronic band structure (changing the resonance conditions). Precise theoretical or experimental band structure information is, however, currently not available.

We made an attempt to evaluate the eventual impact on the observed two-phonon scattering of LO phonons with nonzero wave vectors by calculating the partial density of some states from shell-model dispersion curves. First we calculated the dispersion curves in z direction (each consisting of 400 equidistant points), beginning from the four B_{1u} modes (three optical and one acoustic) at the Γ point (see Fig. 3). The parameters used for these calculations were described elsewhere.^{12,16} From the dispersion curves we calculated the two-phonon combination density of states (see Fig. 3). The differences of up to 30 cm^{-1} between the observed and calculated frequencies of the B_{1u} LO modes are reason-

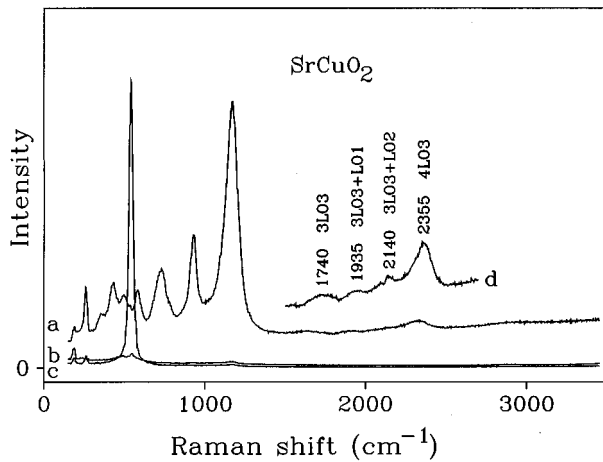


FIG. 4. Room-temperature polarized Raman spectra of SrCuO_2 : (a) $x(zz)\bar{x}$; (b) $x(yy)\bar{x}$; (c) $z(xx)\bar{z}$. $\lambda_L=514.5$ nm. The spectra have a common baseline. The inset (d) is part of the $x(zz)\bar{x}$ spectrum at 10 K (shifted).

able for such a model and allow a qualitative comparison. Indeed, as in the experimental spectrum, three nonoverlapping bands are present in the calculated spectrum over 600 cm^{-1} . On the other hand, the width of the two highest calculated bands is so large (more than the measured width of the corresponding lines at low temperatures) that scattering by zone-boundary phonons should be observable as additional lines in experimental spectrum. Their absence (except the weak features around 790 and 1060 cm^{-1}) confirms the predominant impact of long-wave phonons, i.e., the Fröhlich mechanism of this scattering.

We also note that scattering processes of order $l>2$ were observed for light polarized along the chains [Fig. 4(a) and 4(d)]. It turns out that the position of the peaks above 1500 cm^{-1} is very close to (actually slightly below) triple and quadruple combinations of LO modes. The situation is thus similar to the well-known multiple-phonon scattering in polar semiconductors.¹⁷ In $\text{Sr}_{1-x}\text{Ca}_x\text{CuO}_2$ we observed not only overtones (3LO3 at 1740 cm^{-1} and 4LO3 at 2355 cm^{-1} at 10 K) but also combinational lines. The relative intensity of the latter increase with the scattering order l due to the increase of the topologically inequivalent diagrams for the scattering process.¹⁸ This is the reason for the similar intensities of the 3LO3 overtone at 1740 cm^{-1} and the fourth-order combinations, e.g., 3LO3+LO1 (1935 cm^{-1}) and 3LO3+LO2 (2140 cm^{-1}).

In conclusion, we presented polarized Raman spectra of $\text{Sr}_{1-x}\text{Ca}_x\text{CuO}_2$ ($x = 0, 0.5$). The analysis of the frequencies and the temperature behavior of a series of peaks which are not Raman allowed and observed for polarizations parallel to the Cu-O chains, are explained consistently as Fröhlich-interaction-induced infrared-active B_{1u} LO modes and their combinations. Hence it is not necessary to involve non-phononic mechanisms for their description. The observation of a scattering due to magnetic excitations in these 1D anti-ferromagnets remains an open task.

We thank L. Filippidis for the technical assistance. M.V.A. and A.P.L. acknowledge the financial support from the Alexander von Humboldt Foundation (Bonn, Germany) and from the European Community (ERBCHICT-941659), respectively. They thank the Institut für Festkörperphysik (TU-Berlin) for its hospitality. This work is supported in part by Grant F530 (NIS 2241) of the Bulgarian National Science Fund.

*Permanent address: Faculty of Physics, Sofia University, BG-1126 Sofia, Bulgaria.

- ¹ T. Ami, M. K. Crawford, R. L. Harlow, Z. R. Wang, D. C. Johnston, Q. Huang, and R. W. Erwin, *Phys. Rev. B* **51**, 5994 (1995).
- ² N. Motoyama, H. Eisaki, and S. Uchida, *Phys. Rev. Lett.* **76**, 3212 (1996).
- ³ H. Suzuura, H. Yasuhara, A. Furusaki, N. Nagaosa, and Y. Tokura, *Phys. Rev. Lett.* **76**, 2579 (1996).
- ⁴ O. V. Misochko, S. Tajima, C. Urano, H. Eisaki, and S. Uchida, *Phys. Rev. B* **53**, R14 733 (1996).
- ⁵ M. Yoshida, S. Tajima, N. Koshizuka, S. Tanaka, S. Uchida, and S. Ishibashi, *Phys. Rev. B* **44**, 11 997 (1991).
- ⁶ G. A. Zlateva, V. N. Popov, M. Gylmezov, L. N. Bozukov, and M. N. Iliev, *J. Phys. Condens. Matter.* **4**, 8543 (1992).
- ⁷ S. Sugai, *Phys. Rev. B* **39**, 4306 (1989).
- ⁸ E. T. Heyen, J. Kircher, and M. Cardona, *Phys. Rev. B* **45**, 3037 (1992).
- ⁹ M. Yoshida, S. Tajima, N. Koshizuka, S. Tanaka, S. Uchida, and

T. Itoh, *Phys. Rev. B* **46**, 6505 (1992).

- ¹⁰ T. Uzumaki, K. Hashimoto, and N. Kamehara, *Physica C* **202**, 175 (1992).
- ¹¹ M. Reedyk, C. Thomsen, M. Cardona, J. S. Xue, and J. E. Greedan, *Phys. Rev. B* **50**, 13 762 (1994).
- ¹² M. V. Abrashev, A. P. Litvinchuk, C. Thomsen, and V. N. Popov, *Phys. Rev. B* (to be published).
- ¹³ C. L. Teske and H. Müller-Buschbaum, *Z. Anorg. Allg. Chem.* **379**, 234 (1970).
- ¹⁴ R. S. Roth, C. J. Rawn, J. J. Ritter, and B. P. Burton, *Am. Ceram. Soc.* **72**, 1545 (1989).
- ¹⁵ A. Garcia-Cristobal, A. Cantarero, C. Trallero-Giner, and M. Cardona, *Phys. Rev. B* **49**, 13 430 (1994).
- ¹⁶ V. N. Popov, *J. Phys., Condens. Matter.* **7**, 1625 (1995).
- ¹⁷ J. F. Scott, R. C. C. Leite, and T. C. Damen, *Phys. Rev.* **188**, 1285 (1969).
- ¹⁸ M. Ya. Valakh, A. A. Klochikhin, and A. P. Litvinchuk, *Sov. Phys. Solid State* **26**, 1558 (1984).